

THE UDF05 FOLLOW-UP OF THE HUDF: II. CONSTRAINTS ON REIONIZATION FROM Z-DROPOUT GALAXIES¹

P. A. Oesch², C. M. Carollo², M. Stiavelli³, M. Trenti³, L. E. Bergeron³, A. M. Koekemoer³, R. A. Lucas³, C. M. Pavlovsky³, S. V. W. Beckwith³, T. Dahlen³, H. C. Ferguson³, Jonathan P. Gardner⁴, S. J. Lilly², B. Mobasher³, N. Panagia^{3,5,6}

Draft version February 20, 2024

ABSTRACT

We detect three (plus one less certain) z_{850} -dropout sources in two separate fields (HUDF and NICP34) of our UDF05 HST NICMOS images. These $z \gtrsim 7$ Lyman-Break Galaxy (LBG) candidates allow us to constrain the Luminosity Function (LF) of the star-forming galaxy population at those epochs. By assuming a change in only M^* and adopting a linear evolution in redshift, anchored to the measured values at $z \sim 6$, the best-fit evolution coefficient is found to be 0.43 ± 0.19 mag per unit redshift (0.36 ± 0.18 , if including all four candidates), which provides a value of $M^*(z = 7.2) = -19.7 \pm 0.3$. This implies a drop of the luminosity density in LBGs by a factor of ~ 2.5 over the 170 Myr that separate $z \sim 6$ and $z \sim 7$, and a steady evolution for the LBG LF out to $z \sim 7$, at the same rate that is observed throughout the $z \sim 3$ to 6 period. This puts a strong constraint on the star-formation histories of $z \sim 6$ galaxies, whose ensemble star-formation rate density must be lower by a factor 2 at 170 Myr before the epoch at which they are observed. In particular, a large fraction of stars in the $z \sim 6$ LBG population must form at redshifts well above $z \sim 7$. The rate of ionizing photons produced by the LBG population decreases consistently with the decrease in the cosmic star formation rate density. Extrapolating this steady evolution of the LF out to higher redshifts, we estimate that galaxies would be able to reionize the universe by $z \sim 6$, provided that the faint-end slope of the $z > 7$ LF steepens to ~ 1.9 , and that faint galaxies, with luminosities below the current detection limits, contribute a substantial fraction of the required ionizing photons. This scenario gives however an integrated optical depth to electron scattering that is ~ 2 below the WMAP-5 measurement. Therefore, altogether, our results indicate that, should galaxies be the primary contributors to reionization, either the currently detected evolution of the galaxy population slows down at $z \sim 7$, or the LF evolution must be compensated by a decrease in metallicity and a corresponding increase in ionization efficiency at these early epochs.

Subject headings: galaxies: evolution | galaxies: formation | galaxies: high-redshift | galaxies: luminosity function

1. INTRODUCTION

One of the most fundamental open issues in observational cosmology is what sources reionized the early Universe. Since the $z \sim 6$ quasar Luminosity Function (LF) is found to be too shallow to provide enough ionizing photons (e.g. Fan et al. 2001; Meiksin 2005; Shankar & Mathur 2007), the most likely culprits are thought to be galaxies. A key question is therefore, how the star-forming galaxy population evolves beyond the putative end of reionization at $z \sim 6$, i.e., well into the epoch of reionization.

Direct searches for Ly emission provide a powerful

way to study high-redshift galaxies (e.g. Iye et al. 2006; Stark et al. 2007; Ota et al. 2008); however, it is difficult to estimate the (continuum and) ionizing flux of Ly emitters, and thus their contribution to reionization. A more fruitful approach is provided by the Lyman break technique.

Thousands of Lyman-break galaxies (LBGs) have been identified between $z \sim 3$ and 6 from optical images, providing an estimate for the rest-frame UV LF at those redshifts (e.g. Oesch et al. 2007, hereafter O07; Bouwens et al. 2007, hereafter B07; see also Steidel et al. 1999; Sawicki & Thompson 2006; Yoshida et al. 2006; Iwata et al. 2007). The evolution of the LBG LF throughout this redshift range is however still being debated: especially at the bright end, the strong clustering of bright galaxies and the tiny area coverage of space-based images prevent setting strong constraints on the LF. Another important factor is that the number of spectroscopically confirmed LBGs is still small due to the faintness of the sources. Within these caveats, O07 and B07 have published independent, self-consistent analyses, which agree on a remarkably steady evolution of $M^* \sim 0.35$ mag per unit redshift over the $z = 3$ –6 epoch.

At redshifts $z > 6$, the rest-frame Ly line shifts into the near-infrared (NIR) and the relatively low efficiency

¹ Mostly based on data obtained with the Hubble Space Telescope operated by AURA, Inc. for NASA under contract NAS5-26555. Partly based on data from the Spitzer Space Telescope operated by Jet Propulsion Laboratory, California Institute of Technology under NASA contract 1407.

² Department of Physics, Institute of Astronomy, Eidgenössische Technische Hochschule (ETH Zurich), CH-8093 Zurich, Switzerland; poesch@phys.ethz.ch

³ Space Telescope Science Institute, Baltimore, MD 21218, United States

⁴ Laboratory for Observational Cosmology, Code 665, NASA's Goddard Space Flight Center, Greenbelt MD 20771

⁵ INF-Osservatorio Astronomico di Catania, Via S. Soa 78, I-95123 Catania, Italy

⁶ Supernova Ltd., OYV 131, Northsound Road, Virgin Gorda, British Virgin Islands

and small field of view of current NIR detectors have limited the identification of LBGs. Thus, in contrast to the large number of sources detected out to $z \sim 6$, the numerous searches for $z \gtrsim 7$ LBGs have led to only a handful of candidates (e.g. Bouwens et al. 2008, hereafter B08; Mannucci et al. 2007; Bouwens & Illingworth 2006; Yan & Windhorst 2004; Stanway et al. 2008). Searches for intrinsically faint $z \gtrsim 7$ LBGs around lensing clusters also resulted only in small numbers of candidates (e.g. Richard et al. 2006; Bradley et al. 2008; Richard et al. 2008), due to the small areas subject to the lensing magnification.

One of the most comprehensive studies is the recent analysis of B08, who have measured the $z \sim 7$ LBG LF from a large compilation of both HST and ground-based data, covering a total area of $\sim 271 \text{ arcmin}^2$ over the two fields of the GOODS survey (Giavalisco et al. 2004). Again within the caveats imposed by probing, with small number statistics, only the bright-end of the LF, these authors report that the dimming of the LBG LF which has been measured out to $z \sim 6$ continues with no substantial change out to $z \sim 7$.

A summary of the previous work in the context of reionization is that, albeit within some restrictive assumptions, the detected $z \sim 6$ LBG population appears to be just barely able to maintain the Universe ionized (e.g. Ferguson et al. 2002; Lehnert & Bremer 2003; Stiavelli et al. 2004; Bunker et al. 2004; Bouwens & Illingworth 2006; Gnedin 2008a), and also the detected $z \sim 7$ LBGs fall short of being able to provide the photons required to reionize the Universe (Bolton & Haehnelt 2007). It seems that fainter galaxies must have played a very important role (e.g. Yan & Windhorst 2004; Richard et al. 2008).

Here we present our independent derivation of constraints on the $z \sim 7$ LBG LF. This is desirable in order to independently check the different effects of various uncertainties in the process of estimating LFs, including the data reduction, object detection as well as estimation of effective selection volume. We use our UDF05 data as well as the optical (Beckwith et al. 2007) and NIR (Thompson et al. 2005) data of the Hubble Ultra Deep Field (HUDF). The UDF05 survey is a 204-orbit HST Large Program of ultra-deep ACS and NICMOS observations of multiple fields, each located $10'$ away from HUDF (see O'07). The UDF05 was designed to image with ACS-WFC the two NICMOS parallel fields (hereafter N1CP12 and N1CP34) that were acquired while the HUDF was observed with the ACS and thus facilitating a reliable search for $z > 6$ galaxies in these fields to unprecedented depth.

The combined NIR NICMOS dataset that we study in this paper consists of three fields, covering a total area of 7.9 arcmin^2 , with 5 point-source magnitude limits varying between 27.9–28.8 in F160W (H_{160}) and 27.6–28.6 in F110W (J_{110}). The 50% completeness limits vary between 26.9 and 28.1 mag (see Tab. 1 and x3.1). Each of the fields consists of one deep pointing and a slightly shallower anking area (by 0.6 mag). These data, also used in B08, provide the deepest NIR data available to date.

In x2 we describe the data and the steps adopted to identify the $z \sim 7$ LBG candidates and constrain the LBG LF. In x3 we present our results and their impli-

TABLE 1
Depth and Area of the UDF05 and HUDF NICMOS Observations

Field	5 ^a Z ₈₅₀	5 J ₁₁₀	5 H ₁₆₀	C _{50%} ^b H ₁₆₀	Area arcmin ²
N1CP34 deep	28.3	28.6	28.8	28.1	0.7
N1CP34 shallow	28.2	27.9	28.1	27.3	0.4
N1CP12 deep	28.4	28.4	28.6	27.8	0.7
N1CP12 shallow	28.4	27.8	28.0	27.3	0.4
HUDF deep	28.6	28.2	28.2	27.5	0.7
HUDF shallow	28.6	27.6	27.6	26.9	5.0

^a within an aperture of $0''.3$ radius

^b 50% completeness limit, as estimated in section x3.1

cation for the evolution of the LBG LF into the reionization epoch, and in x4 we discuss the contribution of the detected $z \sim 7$ galaxies to reionization. We adopt the concordance cosmology defined by $\Omega_M = 0.3$; $\Omega_\Lambda = 0.7$; $H_0 = 70 \text{ km s}^{-1} \text{ Mpc}^{-1}$, i.e. $h = 0.7$. Where necessary we assume $\Omega_b h^2 = 0.02265$ (Hinshaw et al. 2008). Magnitudes are given in the AB system (Oke & Gunn 1983).

2. OBSERVATIONS AND SOURCE SELECTION

2.1. The UDF05 and HUDF data

We reprocessed the HUDF data using improved data reduction algorithms relative to the publicly released data, including an iterative sky subtraction scheme. All NICMOS data were drizzled to a $0''.09$ pixel scale. The optical ACS data were rebinned to this same scale and convolved with a Gaussian filter to match the width of the NICMOS point spread function (PSF). We used the H_{160} -band data to detect galaxies with the SExtractor program (Bertin & Arnouts 1996), and measured their colors in elliptical apertures scaled to 1.5 their Kron radii, matched to the detection in age. Total magnitudes were measured in 2.5 Kron (AUTO) apertures and were corrected for flux losses in the wings of the PSF ($0.07 - 0.10 \text{ mag}$).

Only detections with signal-to-noise ratio (S/N) larger than 4.5 within $0''.3$ radius apertures in the H_{160} -band were considered. Flux variations in apertures of different sizes, laid down on empty (sky) areas, were estimated in order to correct for pixel-to-pixel noise correlation in the images; the rms maps were then rescaled so as to match the noise in $0''.3$ radius apertures. Undetected fluxes were replaced with their 1st upper limits. The zeropoints of the J_{110} and H_{160} filters were corrected by 0.16 and 0.04 mag, respectively, in order to account for non-linearity of the NICMOS NIC3 detector (see de Jong 2006). Note that any additional effect of detector non-linearity would be minimal as our sample covers only a small range in magnitudes.

2.2. The z_{850} -dropout candidates

Candidate galaxies at redshifts between 6.8 and 8 were selected from the SExtractor catalog according to the following color criteria:

$$(z_{850} - J_{110}) > 1.3$$

$$(z_{850} - J_{110}) > 1.3 + 0.4 (J_{110} - H_{160})$$

$$(J_{110} - H_{160}) < 1.2$$

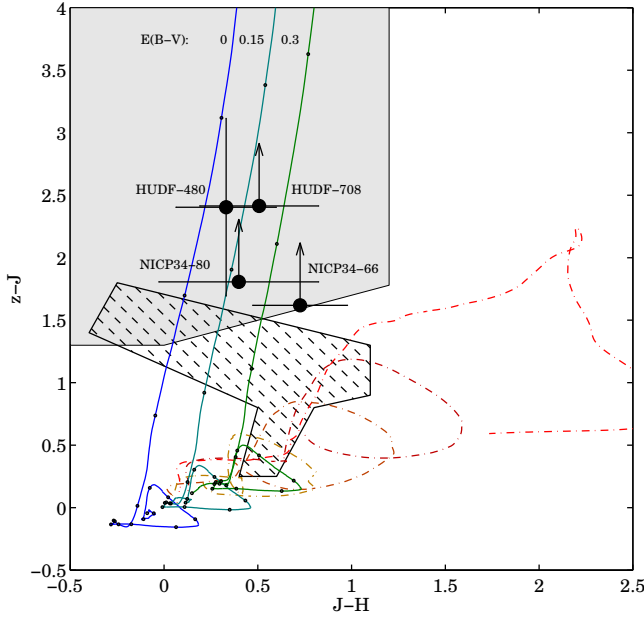


Fig. 1. The $z-J$ vs. $J-H$ color-color diagram, on which we highlight the selection criterion for $z > 6.8$ galaxies (gray shaded area). Evolutionary tracks of star-forming galaxies, obtained with Bruzual & Charlot (2003) models, are shown with solid lines in blue-to-green colors, corresponding to dust obscurations of $E(B-V) = 0; 0.15; 0.3$ mag, respectively (using the extinction law of Calzetti et al. 2000). Low redshift galaxy tracks, up to redshift $z = 4$, are obtained from the galaxy templates of Coleman et al. (1980), and are shown as dash-dotted tracks in orange-to-red colors. Dwarf stars are expected to lie in the hatched region (Knap et al. 2004, Burrows et al. 2006, Pickles 1998). The filled black circles correspond to the four $z > 7$ candidate galaxies identified in our UDF05+HUDF dataset.

$$\begin{aligned} S/N(H_{160}) > 4.5 \quad \wedge \quad S/N(J_{110}) > 2 \\ S/N(V_{606}) < 2 \quad \wedge \quad S/N(i_{775}) < 2 \end{aligned}$$

This selection is indicated as a gray shaded region in the $z-J$ vs. $J-H$ color-color diagram of Fig. 1. The figure also shows tracks of different galaxy types as a function of redshift. A star-forming galaxy with metallicity $0.2Z_{\odot}$ and a stellar age of 10^8 yr is shown with three blue-to-green solid lines, corresponding to $E(B-V) = 0; 0.15; 0.3$ mag, respectively (using the extinction law of Calzetti et al. 2000). Such star-forming galaxies enter the selection window at $z \sim 6.8$. Lower redshift galaxies are shown with dash-dotted lines in orange-to-red colors. The hatched region in the diagram corresponds to the expected location of cool dwarf stars of type M to L (Knap et al. 2004⁷, Burrows et al. 2006, Pickles 1998).

Note that the color selection that we have adopted in this study is the so-called “conservative” criterion in Bouwens & Illingworth (2006). Relative to the less restrictive color window that is used in B08, our selection criterion slightly reduces the effective selection volume by excluding galaxies with redshifts between $z \sim 6.5$ and $z \sim 6.8$; however, it is more robust against low redshift interlopers, and in particular it excludes more efficiently a possible contamination by passively-evolving $z \sim 1.7$ galaxies with a pronounced 4000 Å break.

⁷ We have used the theoretical models of Burrows et al. 2006 to convert the photometry of Knap et al. to the ACS/NICMOS filter set.

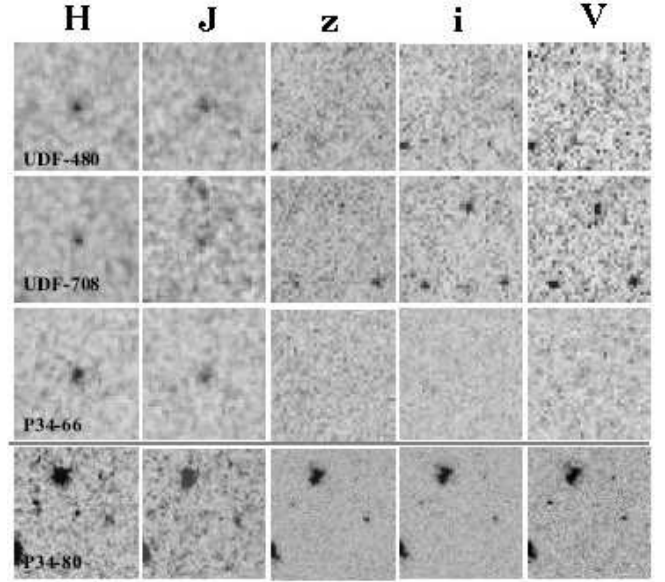


Fig. 2. Images of four z_{850} -dropout candidates. The boxes are $3''.5$ in size. Left to right, the columns show images in H_{160} , J_{110} , z_{850} , i_{775} , and V_{606} . The sources are very compact. All but the faintest candidate (NICP34-80) are securely detected both in H_{160} and J_{110} .

All SE extractor sources that satisfy the above color criterion were visually inspected; four $z > 6.8$ LBG candidates were identified after removal of spurious detections (e.g., stellar diffraction spikes, edge artifacts, etc.). These four high- z galaxy candidates are shown as filled black circles in the color-color diagram of Fig. 1. Images of these sources are shown in Fig. 2; their photometry is listed in Table 2. All four z -dropouts are rather faint ($H_{160} \sim 27$) and very compact (they are essentially unresolved at the resolution of the NICMOS images). Two of the candidates lie in the shallowanking region of the HUDF; the remaining two are located in the shallower area of the NICP34 data. As evident from Fig. 1, three out of our four high- z candidates support relatively small amount of dust, $E(B-V) = 0.15$, while the last one (NICP34-66) is consistent with slightly larger extinction.

Three of our four sources are securely detected in both J_{110} and H_{160} . The faintest source (NICP34-80) has a S/N of 4.8 in the $0''.3$ H_{160} aperture, and of only 2 in the J_{110} aperture. Thus NICP34-80 is a less secure high- z candidate. With the exclusion of NICP34-80, the remaining three objects are also found in the independent analysis of B08. One of the z_{850} -dropouts in our analysis (HUDF-480) had already been reported in previous works (Bouwens et al. 2004b; Bouwens & Illingworth 2006; Coe et al. 2006), and it has also been detected in Spitzer images (Labbe et al. 2006), with infrared colors in very good agreement with a star-forming galaxy at $z \sim 7$. The remaining z_{850} -dropouts in our sample are either undetected (< 2 ; NICP34-66/80) or severely blended (HUDF-708) in the existing, publicly available Spitzer data (from the IRAC followup of GOODS for the HUDF⁸ and from the SIMPLE survey for NICP34⁹).

⁸ <http://data.spitzer.caltech.edu/popular/goods/>

⁹ <http://data.spitzer.caltech.edu/popular/simple/>

TABLE 2
Photometry of the four z_{850} -dropout sources

ID			H_{160}	S/N (H_{160})	$J_{110}-H_{160}$	$z_{850}-J_{110}$	FWHM
HUDF-480	3:32:38.81	-27:47:07.2	26:9	0:1	7.2	0:3 0:3	2:4 0:7 0 ⁰ 30
HUDF-708	3:32:44.02	-27:47:27.3	27:3	0:2	6.8	0:5 0:3	> 2:4 0 ⁰ 29
NICP 34-66	3:33:08.29	-27:52:29.2	26:9	0:1	12.5	0:7 0:3	> 1:6 0 ⁰ 54
NICP 34-80 ^a	3:33:10.63	-27:52:31.0	27:8	0:2	4.8	0:4 0:4	> 1:8 0 ⁰ 35

^a This object could be a spurious detection. We have detected it with a 2 σ significance in J_{110} , and it has not been confirmed by an independent reduction of the same data by R. Bouwens (2008, private communication).

The magnitude limits for the sources in NICP 34 are quite bright and thus do not add any constraint on their photometric redshifts.

2.3. Sources of sample contamination

There are five possible sources of contamination to the derived sample of $z \sim 7$ galaxy candidates; these are due to (i) spurious detections, (ii) cool dwarf stars, (iii) low redshift galaxies with colors similar to $z \sim 7$ galaxies, (iv) high redshift supernovae, and (v) photometric scatter of low redshift galaxies into our selection window. In detail:

(i) Except for the faintest of our sources, NICP 34-80, all candidates are detected at more than 6 σ in H_{160} and $> 3\sigma$ in J_{110} . It is therefore very unlikely that these high S/N sources are produced by peaks in the noise. In order to estimate the reality of NICP 34-80, which is only detected at 2 σ in J_{110} , we repeated our analysis on ‘negative images’, obtained by multiplying the real images by -1 (after masking out all detected sources). One ‘negative source’ is detected with $S/N(H_{160}) > 4.5$, $S/N(J_{110}) > 2$ and a pixel flux distribution similar to NICP 34-80. Thus, we conclude that NICP 34-80 is likely a spurious detection.

(ii) Except for NICP 34-66, whose profile has a full-width-half-maximum (FWHM) of 0⁰54, all sources are unresolved (FWHM 0⁰29–0⁰35; see Table 2). For comparison, stars are measured to have FWHM of 0⁰30–0⁰39 (see also Thompson et al. 2005). Thus, on the basis of their profiles, we cannot exclude the possibility that our candidates are stars. However, they all show colors redder than expected for ultracool dwarfs. Such stars should have at least weak detections in our ultra-deep z_{850} data. Therefore it is unlikely that our candidates are dwarf stars. However, simulations of dwarf star LFs by Burgasser (2004) predict that there will be ~ 0.5 stars of type L0–T8 in our survey in the magnitude range of $H_{AB} = 27–28$. Thus, this is a non-negligible source of contamination.

(iii) Galaxies at $z \sim 1.2–1.8$ which emit a combination of a red continuum (due to dust or old stellar age) and strong [O III] 5007, 4959 and H α emission lines can exhibit colors which place them within our selection window. The equivalent widths of the emission lines that are required are however rather extreme (~ 500 Å rest-frame), which makes this a rather implausible source of contamination.

(iv) The 2.2 arcmin² NICMOS observations for the UDF05 data were taken at a much earlier epoch than the corresponding ACS images; high redshift SNe could therefore also contaminate our sample. However, with a similar calculation as in B08, we expect to find only 0.03

SNe within the area of our NICMOS observations; this is thus a negligible source of contamination in our sample.

(v) Photometric scatter could in principle cause some contamination as well. In particular, $z \sim 1.7$ galaxies with prominent 4000 Å breaks, the closest to our selection window, could be a significant source of contamination. In order to assess the importance of this effect, we run simulations in which we applied a suitable photometric scatter to the HUDF source catalog of Coe et al. (2006). This catalog contains sources separately identified both in the optical and in the infrared, and includes one of our $z \sim 7$ candidates. The catalog also contains photometric redshifts for all sources. We can thus study the redshift distribution of galaxies which enter our selection window after applying the photometric scatter. Certainly this test is limited by the reliability of the photometric redshifts. However, it provides a worthy cross check on our candidates, and we found no low redshift source in any of the simulation runs. In general, requiring that an object is not detected in any of the optical bands efficiently reduces the contamination from lower redshift interloper galaxies.

In summary, three of the four detected z_{850} -dropouts are very likely to be genuine $z \sim 7$ LBGs. However, we stress that future observations will be needed to confirm these candidates as high- z sources. In the following we discuss the implications for galaxy formation and reionization of assuming that these three objects are truly galaxies at $z \sim 7$; we also separately comment on the impact of including the fourth, less likely high- z candidate in our $z \sim 7$ LBG sample.

3. RESULTS

3.1. Expected vs. detected number of sources

In order to estimate the completeness, C , and redshift selection probability, S , for our sample, we used the procedure that we outlined in Oesch et al. (2007), i.e., we simulated data by inserting artificial galaxies into the real images, and run SExtractor on the simulated data with the same parameters adopted to extract the original catalogs. We adopted colors according to a Gaussian distribution of continuum slopes that is measured for $z \sim 6$ LBGs ($\beta = 2.2 \pm 0.2$; Stanway et al. 2005), and a log-normal size distribution with a size scaling of $(1+z)^{-1}$ (Ferguson et al. 2004; Bouwens et al. 2004a).

Given a LF, the number of objects expected in a bin of a given magnitude, Δm , is given by

$$N(\Delta m) = \int_{\text{bin}} \frac{dN}{dm} \frac{dz}{dz} \frac{dV}{dz} (M[\ln^0; z]) S(z; m^0) C(m^0)$$

where $M[\ln^0; z] = m - K(z)$ and $DM(z)$ is the absolute

magnitude, m the observed magnitude, $K(z)$ the K -correction term and DM the distance modulus. We adopted a 10^8 yr old, 0.2Z, star-forming template for the K -correction from the observed H_{160} -band to rest-frame 2000 Å, with $E(B-V) = 0.15$, consistent with best-fit SEDs for $z \sim 5$ LBGs (e.g. Verma et al. 2007). Note that correcting to 1400 Å results in a difference of only 0.07 mag. The total number of expected $z \sim 7$ galaxies in our survey is then just the sum over all the fields, which all have different selection probabilities and completenesses due to the different depths and data quality.

Assuming no evolution in the LF from $z \sim 6$ to 7, we would expect to detect 12 galaxies in our dataset (using the $z \sim 6$ parameters of B07); in contrast, only three, or at most four (if the least reliable candidate, N ICP 34-80, is also included), are detected. In particular, we would expect about four galaxies brighter than $H_{160} < 26.75$. No such bright candidate is observed, which leads us to conclude, albeit with a limited significance, that there is evolution in the LBG LF from $z \sim 6$ to $z \sim 7$. From Poissonian statistics, the detection of four sources out of the expected 12 has a significance of 2.3; when cosmic variance is considered¹⁰, the significance of the result is reduced down to 1.4. The same, i.e. a chance of 8%, is found from accurate beam tracing through a dark matter simulation in which halos are populated with galaxies taking into account the specific geometry of our survey (Trenti & Stiavelli 2008). Note however that, as commented above, the N ICP 34-80 source is likely a spurious detection; should this or any other high- z candidate in our sample turn out to be an artifact (or a lower redshift interloper), this would imply a stronger evolution of the LF over the $z \sim 6$ out to $z \sim 7$ period. The estimates above therefore provide a lower limit to the real evolution of the LF across the reionization boundary.

3.2. The $z \sim 7$ LBG luminosity function

The approach that we use to constrain the $z \sim 7$ LBG LF from our data is to fix the faint-end slope and the normalization, and search for evolution in M only; this approach is motivated by the finding that M is the only LF parameter which substantially varies over the $z \sim 4$ – 6 redshift range (B07). We adopt a linear evolution $M(z) = M(z = 5.9) + (1+z)$ and treat the only free parameter, α , to our four (three) $z \sim 7$ candidates. We use the parameters of B07 to anchor the evolution at redshift 5.9, i.e. we adopt $\alpha(z = 5.9) = 1.4 \times 10^{-3} \text{ Mpc}^3 \text{ mag}^{-1}$, $\alpha(z = 5.9) = 1.74$, and $M(z = 5.9) = 20.24 \pm 0.19$.

To determine α , we maximize the likelihood

$$L = \prod_i P[N_{\text{obs}}(m_i); N_{\text{exp}}]$$

where $P[x; \lambda]$ is the Poisson distribution with mean evaluated at x ; $N_{\text{obs}}(m_i)$ is the observed number of objects in the magnitude bin m_i , and N_{exp} are the expected number of objects for a given evolution parameter α .

The best fit for α is 0.36 ± 0.18 , which translates into $M(z = 7.2) = 19.77 \pm 0.30$. If we exclude the

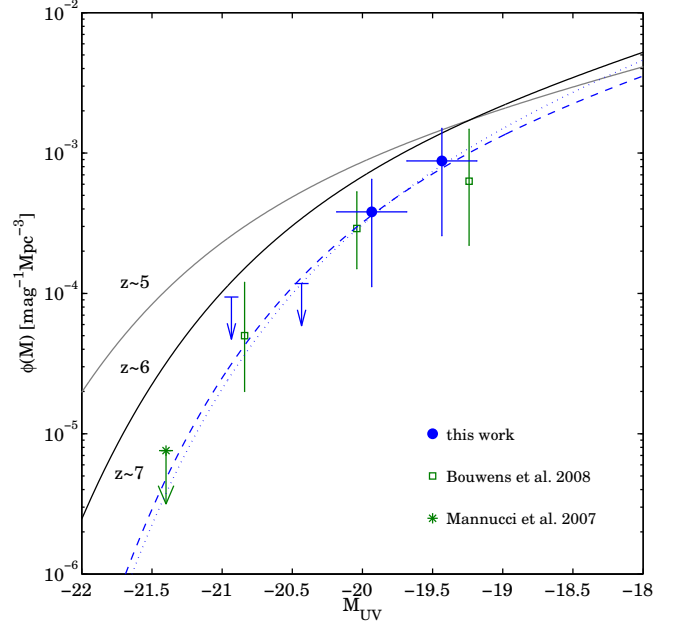


Fig. 3. The $z \sim 7.2$ LBG LF derived from our four candidates (filled blue circles). The best-fit Schechter function, derived from maximizing the likelihood for the evolution parameter α , is shown as a dashed line. The dotted line is the same, but with a steeper faint-end slope $\alpha = 1.9$. Upper limits for empty magnitude bins are indicated with blue arrows. Open squares are from Bouwens et al. (2008), with whom we have three high- z candidates in common. The upper limit at $M = -21.4$ is from Mannucci et al. (2007). The other lines show the LF at $z \sim 5$ (gray solid line; Oesch et al. 2007), and $z \sim 6$ (black solid line; Bouwens et al. 2007).

faintest, least reliable z_{850} -dropout candidate from the list, the result changes only slightly, i.e., $\alpha = 0.43 \pm 0.19$, or $M(z = 7.2) = 19.68 \pm 0.31$. Within the errors these values are identical, and we adopt a fiducial value of $M(z = 7.2) = 19.7 \pm 0.3$ at 2000 Å. With this evolving LF, the redshift distribution of our sources is predicted to be $z = 6.8 \pm 7.7$ (within the 16th and 84th percentiles), with a mean $\bar{z} = 7.2$. The resulting LF is shown in Fig. 3 as a dashed line; the figure assumes that all candidates lie at $z_{R172} = 7.2$, with the effective volume estimated as $V_e(m) = \int_0^{\infty} dz \frac{dV}{dz} S(z; m) C(m)$.

Since the measured evolution is mostly driven by the non-detection of bright sources, the effect of varying the faint-end slope is very small. Varying α by 0.16 (the formal 1- σ error of the $z \sim 6$ LF) changes the value of $M(z = 7.2)$ by only 0.03 mag. We have also tested how the LF would evolve if M does not evolve while α varies with redshift; this would result in a value a factor 2.5 lower than at $z \sim 6$, i.e., $\alpha = (0.56 \pm 0.50) \times 10^{-3}$.

B08 used a large sample of NIR data, covering an area of 261 arcmin² (including the ultra-deep N ICMOS data of this work) and found $M = 19.8$ and $\alpha = 1.1 \times 10^{-3} \text{ mag}^{-1} \text{ Mpc}^3$, in very good agreement with our result (see also Fig. 3). Furthermore, Mannucci et al. (2007) searched the ground-based VLT/ISAAC J, H, and Ks data on the GOODS field for z_{850} dropouts and, after removing probable dwarf stars, they found no candidates down to a UV rest-frame absolute magnitude of $M_{1500} = -21.4$. These authors inferred an upper limit on the LF down to this magnitude which we also report in Fig. 3; this upper limit is in good agreement with the

¹⁰ Our cosmic variance calculator is publicly available at <http://www.stsci.edu/~trenti/CosmicVariance.html>

extrapolation to brighter magnitudes of our $z = 7$ LF.

4. IMPLICATIONS FOR GALAXY EVOLUTION AND REIONIZATION

4.1. Evolution of the star formation rate density and star formation histories of $z = 6$ LBGs

From the above LF we can compute the amount of evolution in the cosmic star formation rate density from $z = 6$ out to $z = 7$. Integrating down to $0.2L$ ($z = 6$), corresponding to $M = -18.5$, we find a decrease in the luminosity density by 50%, i.e., $\log(\epsilon_{\text{erg}} = S_{\text{H}} z = M \text{ pc}^3) = 25.5 - 0.2$. Using the relationship between UV continuum and star formation rate of Kennicutt (1998), this corresponds to a star formation rate density of $10^{-2.32 \pm 0.23} M_{\odot} \text{ yr}^{-1} \text{ Mpc}^{-3}$. Assuming that the LF evolves only in density implies instead a reduction of 60%. Thus, independent from the specific assumption on the LF evolution (either in M or in z), down to this brightness limit the luminosity density, and thus the star formation rate density, drops by a factor of ~ 2.5 over the 170 Myr that separate the $z = 6$ and $z = 7$ epochs. Mannucci et al. (2007) and B08 independently find similar results. Note that the conversion of Kennicutt is applicable for galaxies with continuous star formation over timescales of a few 100 Myr and Salpeter initial mass function (IMF). They might differ for galaxies which are experiencing stochastic bursts, as is assumed for high- z LBGs (Vermi et al. 2007). However, larger differences are expected due to uncertainties in the IMF.

The observed decline of the bright end of the LF from $z = 6$ out to $z = 7$ provides an upper boundary on the ensemble average star formation rate of $z = 6$ LBGs 170 Myr prior to the epoch at which they are observed. Eyles et al. (2007) have investigated the ensemble average star formation history of i_{775} -dropouts brighter than $z_{850} = 27$ in the GOODS field, and suggested that this rises from $z = 6$ to a peak at $z = 7.5$, and declines beyond this redshift. Using Bruzual & Charlot (2003) models and assuming the star formation history of Eyles et al. (2007), we find that the rest-frame 1500 Å luminosity density should show an increase by a factor of ~ 2.5 from $z = 6$ up to 7, i.e., in striking contrast with the drop of the luminosity density that we report above. Dust corrections can not reconcile this disagreement, unless an evolution towards larger dust obscuration at higher redshifts is invoked.

This apparent contradiction could however be an artifact of the specific star formation history that has been adopted by Eyles et al. in the computation of the ensemble average. Generally, Spitzer data of i_{775} -dropouts in the GOODS fields have revealed prominent 4000 Å breaks in a large fraction of these sources ($\sim 40\%$), indicating up to 90% of old stellar populations in those $z = 6$ galaxies (Yan et al. 2005; Eyles et al. 2007). Our results on the $z = 7$ LF provide global support to a scenario where a large fraction of stars in the $z = 6$ population form at redshifts well above $z = 7$.

4.2. Do galaxies reionize our universe?

Consistent with the decrease in cosmic star formation rate density, the rate of ionizing photons produced by LBGs must also decrease between $z = 6$ and $z = 7$.

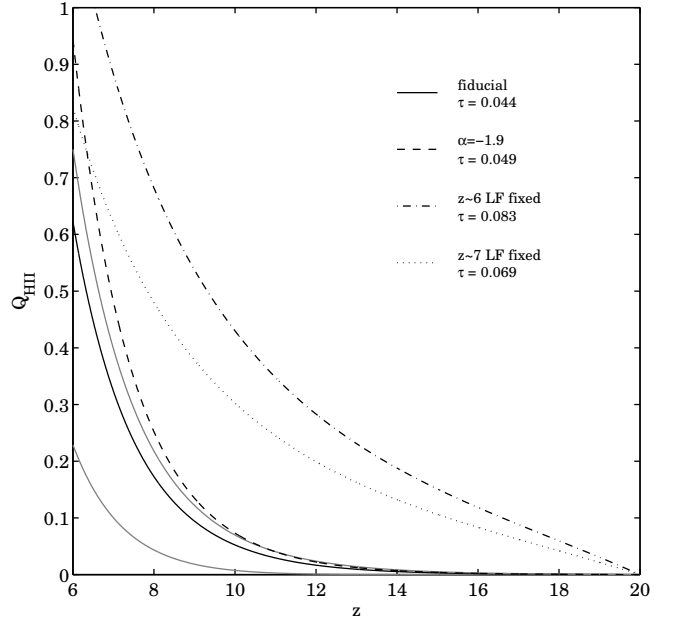


Fig. 4. | Filling factor of ionized hydrogen as a function of redshift. The solid lines show the evolution of the filling factor calculated by assuming a faint end slope $\alpha = -1.74$ and an evolution of the galaxy LF by 0.35 mag per unit redshift, and by integrating down to different limiting SFRs ($1; 0.01; 0.0001 M_{\odot} \text{ yr}^{-1}$; lower gray, black, and upper gray lines, respectively). The dashed line assumes the same evolution in M but $\alpha = -1.9$. The dash-dotted line corresponds to no evolution of the LF from $z = 6$ out to $z = 20$; the dotted one assumes the same but with the $z = 7$ LF. If not stated otherwise all curves are integrated down to SFRs of $10^{-2} M_{\odot} \text{ yr}^{-1}$. The corresponding electron scattering optical depths are also indicated.

Bolton & Haehnelt (2007) pointed out that, with the estimated $z = 7$ LF of Bouwens et al. (2004b), the number of ionizing photons falls short by almost an order of magnitude even to just keep the universe ionized at $z = 7$. Only models in which the star formation rate rises or stays constant beyond $z = 6$ are able to provide enough ionizing photons. This result was however derived by including only galaxies with absolute magnitudes brighter than $M = -18$ mag; this corresponds to a lower limit for the star formation rate of $1 M_{\odot} \text{ yr}^{-1}$ (see lower gray line in Fig. 4). For LF faint-end slopes as steep as those that are measured, however, 50% of the luminosity density comes from galaxies beyond the current detection limits at $z = 6$ ($M > -17$ mag). Thus, photons from these very faint galaxies will add a substantial contribution to the reionizing flux.

Here we adopt the results of our independent analysis of the $z = 7$ LF, which, using substantially improved data products, confirms the drop in the star formation rate density from $z = 6$ to $z = 7$ suggested by Bouwens et al. (2004b). We follow the approach of Bolton & Haehnelt (2007) to estimate the contribution of galaxies to reionization. We include, however, the contribution of faint galaxies to reionization by decreasing the lower limit star formation rate to $10^{-2} M_{\odot} \text{ yr}^{-1}$ in our calculations.

Computations of the filling factor of ionized hydrogen, Q_{HII} , critically depend on the adopted values of the clumping factor C and escape fraction f_{esc} . Scenarios with larger clumping factors lead to more efficient recombinations and thus require more ionizing photons;

lower escape fractions also require more photons. Both the clumping factor and the escape fraction are however poorly known. To give an upper limit on the potential for reionization of the galaxy population, we adopt (possibly somewhat optimistic) values of $C = 2$, as found in simulations (see discussion in Bolton & Haehnelt 2007), and $f_{\text{esc}} = 20\%$, the upper limit that has been inferred from both observations and simulations (e.g. Shapley et al. 2006; Siana et al. 2007; Gnedin et al. 2008b). We neglect any possible mass dependence of f_{esc} .

Assuming (i) that the constant dimming of M_{UV} with redshift continues beyond $z \gtrsim 7$ and (ii) a faint-end slope which remains constant at the value $\alpha = -1.74$ that is measured at $z \lesssim 6$ (i.e., our "fiducial" evolution parameters), the galaxy population would be able to ionize the universe only up to a fraction $Q_{\text{H II}} = 65\%$ (see solid lines in Fig. 4). The corresponding optical depth to electron scattering is $\tau = 0.044$, which is ~ 2.5 lower than the WMAP-5 value of $\tau = 0.087 \pm 0.017$ (Dunkley et al. 2008). Thus, this reionization scenario starts too late, ionizing too few atoms at high redshifts. Indeed the WMAP-5 data suggest that the Universe underwent an extended period of partial reionization, beginning as early as $z \sim 20$, similar to the double reionization scenario proposed by Cen (2003). If by $z \sim 9$ the Universe is already substantially ionized by some other sources, the galaxy population would certainly be able to complete the reionization process by $z \sim 6$.

Another possibility is that the $z > 7$ LF has a faint-end slope which is steeper than currently observed at $z \lesssim 6$ (predicted e.g. by Ryan et al. 2007). The current estimate(s) do not allow one to rule out that the faint end of the LF at such early epochs is as steep as $\alpha = -2$, which would result in a diverging luminosity density. To assess whether the faint galaxy population can provide enough additional photons to complete reionization by $z \sim 6$, we adopt a value of $\alpha = -1.9$ (see dotted line in Fig. 3) and recompute the ionizing factor of neutral hydrogen under these modified assumptions. This scenario is shown in Fig. 4 as a dashed line. Such a steep faint-end slope for

the LF would result in an end of reionization by $z \sim 6$, and in an integrated electron scattering optical depth of $\tau = 0.049$, which is still substantially lower than the current WMAP-5 value. For comparison, we also show in Fig. 4 the evolution of the H II ionizing factor assuming no evolution in the LF from $z \lesssim 6$ ($z \lesssim 7$) to $z = 20$. Integrating the luminosity density again to $10^{-22} \text{ M}_{\odot} \text{ yr}^{-1}$, this results in the completion of reionization by $z \sim 6.6$ (± 0.4) and in an optical depth $\tau = 0.083 \pm 0.069$.

We therefore conclude that: (i) In order for the galaxy population to provide a substantial contribution to reionization, galaxies below current detection limits must play a significant role; (ii) Under this assumption, a galaxy population which evolves by $0.35 \text{ mag per redshift unit}$ would be able to ionize the universe by $z \sim 6$, provided that the LF faint-end slope is steeper than the $\alpha = -1.74$ value that is measured at redshifts $z \lesssim 6$; (iii) Even under this assumption, the resulting optical depth to electron scattering is lower by ~ 2 relative to the WMAP-5 measurement, indicating that too few atoms are ionized at very high redshift. This finding provides evidence that, if reionization is primarily driven by galaxies, either the currently detected evolution of the galaxy population slows down at $z \gtrsim 7$, or the LF evolution is compensated by a decrease in metallicity and a corresponding increase in ionization efficiency (Stiavelli et al. 2004). Otherwise, other sources must substantially participate to reionize our Universe like miniquasars or population III stars (e.g. Shull & Venkatesan 2008; Madau et al. 2004; Sokasian et al. 2004).

Acknowledgements: We wish to thank the anonymous referee for helpful comments that have improved the presentation of these results. P.O. thanks Rychard Bouwens for helpful discussions and for private communication of the result of an independent reduction of the data to establish the reality of our faintest candidate. This work has been partially supported by NASA HST grant 01168.

Facilities: HST (ACS/NICMOS).

REFERENCES

- Ando, M. et al. 2004, *ApJ*, 610, 635
 Beckwith, S. V. W. et al. 2006, *AJ*, 132, 1729
 Bertin, E. and Arnouts, S. 1996, *A & A*, 117, 393
 Bolton, J. S. & Haehnelt, M. G. 2007, *MNRAS*, 382, 325
 Bouwens, R. J. et al. 2004a, *ApJ*, 611, 1
 Bouwens, R. J. et al. 2004b, *ApJ*, 616, L79
 Bouwens, R. J. & Illingworth, G. D. 2006, *Nature*, 443, 189
 Bouwens, R. J. et al. 2007, *ApJ*, 670, 928
 Bouwens, R. J. et al. 2008, *arXiv:0803.0548* (B08)
 Bradley, L. D. et al. 2008, *arXiv:0802.2506*
 Bruzual, G. and Charlot, S. 2003, *MNRAS*, 344, 1000
 Bunker, A. J. et al. 2004, *MNRAS*, 355, 374
 Burgasser, A. J. 2004, *ApJS*, 155, 191
 Burrows, A. et al. 2006, *ApJ*, 640, 1063
 Calzetti, D. et al. 2000, *ApJ*, 533, 682
 Cen, R. 2003, *ApJ*, 591, 12
 Coe, D. et al. 2006, *AJ*, 132, 926
 Coleman, G. D. et al. 1980, *ApJS*, 43, 393
 Dunkley, J. et al. 2008, *arXiv:0803.0586*
 Eyles, L. P. et al. 2007, *MNRAS*, 374, 910
 Fan, X. et al. 2001, *AJ*, 122, 2833
 Ferguson, H. C. et al. 2002, *ApJ*, 569, 65
 Ferguson, H. C. et al. 2004, *ApJ*, 600, 107
 Giallisco, M. et al. 2004, *ApJ*, 600, L103
 Gnedin, N. 2008a, *ApJ*, 673, L1
 Gnedin, N. et al. 2008b, *ApJ*, 672, 765
 Hinchshaw, G. et al. 2008, *arXiv:0803.0732*
 Iwata, I. et al. 2007, *MNRAS*, 376, 1557
 Iye, M. et al. 2006, *Nature*, 443, 186
 de Jong, R. S. 2006, *Instr. Sci. Rep.* 2006-003
 Kennicutt, R. C. 1998, *A & A*, 36, 189
 Knapp, G. R. et al. 2004, *AJ*, 127, 3553
 Labbe, I. et al. 2006, *ApJ*, 649, L67
 Lehnert, M. D. & Bremer, M. 2003, *ApJ*, 593, 630
 Madau, P. et al. 2004, *ApJ*, 604, 484
 Mannucci, F. et al. 2007, *A & A*, 461, 423
 Meiksin, A. 2005, *MNRAS*, 356, 596
 Oesch, P. A. et al. 2007, *ApJ*, 671, 1212 (O07)
 Oke, J. B. and Gunn, J. E. 1983, *ApJ*, 266, 713
 Ota, K. et al. 2008, *ApJ*, 677, 12
 Pickles, A. J. 1998, *PASP*, 110, 863
 Richard, J. et al. 2006, *A & A*, 456, 861
 Richard, J. et al. 2008, *arXiv:0803.4391*
 Ryan, R. E. et al. 2007, *ApJ*, 668, 839
 Sawicki, M. & Thompson, D. 2006, 642, 653
 Shankar, F. & Mathur, S. 2007, *ApJ*, 660, 1051
 Shapley, A. E. et al. 2006, *ApJ*, 651, 688
 Shull, J. M. & Venkatesan, A. 2008, *arXiv:0806.0392*
 Siana, B. et al. 2007, *ApJ*, 668, 62
 Sokasian, A. et al. 2004, *MNRAS*, 350, 47
 Stanway, E. et al. 2005, *MNRAS*, 359, 1184
 Stanway, E. et al. 2008, *MNRAS*, 312, in press
 Stark, D. P. et al. 2007, *ApJ*, 663, 10
 Steidel, C. et al. 1999, *ApJ*, 519, 1
 Stiavelli, M. et al. 2004, *ApJ*, 610, L1
 Thompson, R. I. et al. 2005, *AJ*, 130, 1
 Tremi, M. & Stiavelli, M. 2008, *ApJ*, 676, 767
 Verra, A. et al. 2007, *MNRAS*, 377, 1024

- Yan, H. & Windhorst, R. A. 2004, *ApJ*, 612, L93
Yan, H. et al. 2005, *ApJ*, 634, 109
Yoshida, M. et al. 2006, *ApJ*, 653, 988